Meridiani Planum and the global hydrology of Mars

Jeffrey C. Andrews-Hanna[1]*, Roger J. Phillips[1] & Maria T. Zuber[2]

The Opportunity Mars Exploration Rover found evidence for groundwater activity in the Meridiani Planum region of Mars[1,2] in the form of aeolian and fluvial sediments[3] composed of sulphate-rich grains. These sediments appear to have experienced diagenetic modification in the presence of a fluctuating water table[3–5]. In addition to the extensive secondary aqueous alteration, the primary grains themselves probably derive from earlier playa evaporites[1,2,4]. Little is known, however, about the hydrologic processes responsible for this environmental history—particularly how such extensive evaporite deposits formed in the absence of a topographic basin. Here we investigate the origin of these deposits, in the context of the global hydrology of early Mars, using numerical simulations, and demonstrate that Meridiani is one of the few regions of currently exposed ancient crust predicted to have experienced significant groundwater upwelling and evaporation. The global groundwater flow would have been driven primarily by precipitation-induced recharge and evaporative loss, with the formation of the Tharsis volcanic rise possibly playing a role through the burial of aquifers and induced global deformation. These results suggest that the deposits formed as a result of sustained groundwater upwelling and evaporation, rather than ponding within an enclosed basin. The evaporite formation coincided with a transition to more arid conditions[6] that increased the relative impact of a deep-seated, global-scale hydrology on the surface evolution.

Despite its currently cold and desiccated surface, Mars exhibits abundant evidence for a more clement climate in its early history, with surface temperatures above the freezing point of water and liquid precipitation in the mid-latitudes driving runoff and valley formation[7,8]. Evidence from both the global mineralogy[6] and the geomorphology of valley networks[9–11] points towards a transition from conditions in which water was abundant on the surface early in the Noachian epoch (4.55 to ~3.7 Gyr ago[12]), to more arid conditions late in the Noachian and into the Hesperian epoch (~3.7 to ~3.0 Gyr ago[12]). These arid conditions facilitated the formation of stacks of layered sediments rich in evaporitic sulphate minerals and diagenetic haematite at Meridiani Planum and the associated etched terrain[1–5,13]. The contemporaneous formation of the Meridiani deposits with nearby valley networks[14] and the continued formation of sapping valleys[10] suggest that some precipitation persisted even as the climate became more arid, but quickly infiltrated the surface. This precipitation was the dominant contributor to the groundwater hydrology of early Mars, charging aquifers at high elevations[15] (Fig. 1a) in the southern highlands and on the incipient Tharsis volcanic rise.

The Tharsis rise dominates the topography of the western hemisphere of Mars[15], and played a key role in the global geodynamic and hydrologic evolution[16–19]. Although evidence suggests that the Meridiani deposits are ancient, their exact age and timing relative to Tharsis remains unclear. The Noachian age for the deposits suggested by the crater population[5,20,21], coupled with their formation contemporaneous with nearby valley networks[14] (which generally follow a trend consistent with Tharsis-induced deformation[19]), suggests that they may have formed shortly after or towards the end of Tharsis construction. The formation of Tharsis through a combination of extrusive and intrusive volcanism[16–19] largely during the Noachian[19] would have buried any pre-existing aquifers in the region to depths of the order of 30 km beneath the growing volcanic load[19].
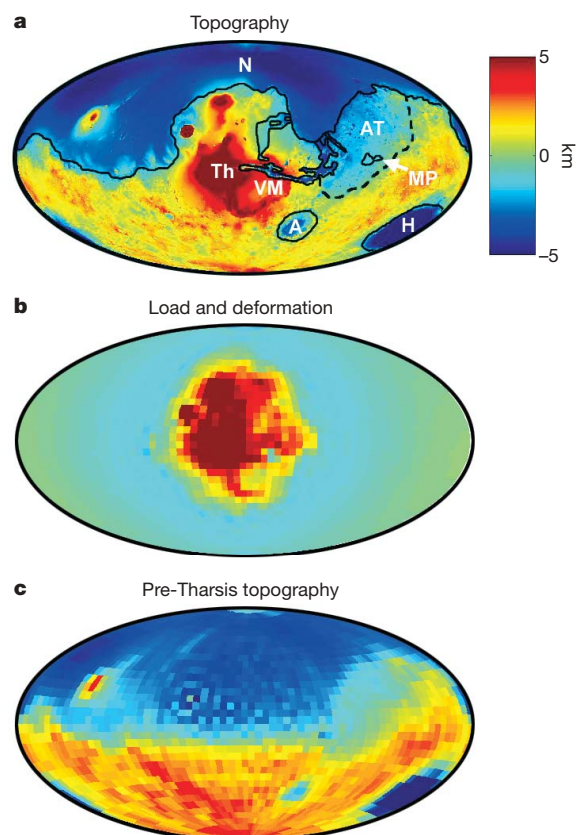

Figure 1 | Topography of Mars and Tharsis-induced deformation. The colour scale applies to all panels. **a,** Topography of Mars from the Mars Orbiter Laser Altimeter, MOLA[15] (Hammer projection centred on 270° E, 0° N). Major features are outlined and labelled, including Tharsis (Th), Valles Marineris canyons (VM), Hellas (H) and Argyre (A) impact basins, the northern lowlands (N), Arabia Terra (AT), and Meridiani Planum (MP). The dashed line represents the break in slope separating Arabia Terra and the southern highlands. **b,** Modelled topography changes due to Tharsis loading and induced deformation (at a resolution of 5° per pixel; assumes a lithosphere thickness of 100 km, Young's modulus of 100 GPa, and Poisson's ratio of 0.25). **c,** Reconstructed pre-Tharsis topography.

[1]McDonnell Center for the Space Sciences and the Department of Earth and Planetary Sciences, Washington University, St Louis, Missouri 63130, USA. [2]Department of Earth, Atmospheric, and Planetary Sciences, Massachusetts Institute of Technology, Cambridge, Massachusetts 02139, USA. *Present address: Department of Earth, Atmospheric, and Planetary Sciences, Massachusetts Institute of Technology, Cambridge, Massachusetts 02139, USA.

A limit on the maximum depth to which aquifers are stable is dictated by the brittle–plastic transition (BPT)[22] due to the loss of porosity and permeability in the plastic regime. During the growth of Tharsis, the BPT would have migrated upwards as the deeply buried portions of the crust approached thermal equilibrium. As the buried aquifers underwent the transition to the plastic regime, the water within would have been placed under the burden of the full lithostatic pressure and been expelled, resulting in a steady upwards flux of water beneath Tharsis (Supplementary Fig. 1). This process is analogous to, though on a much larger scale than, the ejection of water from sediments upon burial and compaction in terrestrial environments[23]. If migration of the BPT lagged behind Tharsis growth, as would be expected for plausible thermal diffusion timescales in the deep crust, aquifers beneath Tharsis would have acted as a net hydrological sink during growth of the rise, and then as a net source of fluid after its completion. In addition, the global membrane-flexural deformation of the planet in response to Tharsis loading would have depressed the lithosphere beneath Tharsis and uplifted the antipodal Arabia bulge[19], driving a net migration of groundwater towards Tharsis[14].

We represent global-scale groundwater flow using the time-dependent, nonlinear Boussinesq equation for hydraulic head (h, measured relative to the geoid) in an unconfined aquifer, with a spatially and temporally varying source term (s) representing the flux of water from both surface precipitation and BPT migration beneath Tharsis (Supplementary equation (1)). The large horizontal length scales relative to the aquifer thickness allow us to reduce the problem to two dimensions, using the vertically averaged hydraulic conductivity (K) and storativity (S) over the active aquifer thickness (d), all functions of the elevation and the hydraulic head[22]. The equation is solved in spherical coordinates (θ,φ), using a fully explicit finite difference approach with a grid resolution of $5°$. We assume semi-arid conditions, in which the water table is not permitted to rise above the surface, simulating evaporative groundwater loss rather than runoff and the formation of large standing bodies of water. The globally integrated evaporative loss is balanced by precipitation distributed uniformly between latitudes of $\pm45°$, consistent with the observed distribution of valley networks.

We consider three possible scenarios for the global hydrological evolution. The 'pre-Tharsis' model assumes that the Meridiani deposits formed before Tharsis, while the 'post-Tharsis' model assumes that Tharsis was a primordial feature of the planet that pre-dated the deposits. We also model the hydrologic evolution with a steady rate of Tharsis construction over 500 Myr, adjusting the hydraulic head to reflect the changing global topography and geoid. The constructional and membrane-flexural changes in the topography and geoid induced by Tharsis formation are calculated using a spherical harmonic loading model[19,24] and subtracted from the present-day values to reconstruct the intermediate stages of Tharsis growth (Fig. 1). The time-dependent migration of the BPT and ejection of water from deep aquifers (Supplementary Fig. 2) is calculated using a one-dimensional finite difference thermal model.

At the end of the simulation in the pre-Tharsis model, the water table intersects the surface across much of the northern lowlands and in the major impact basins, and these are the main concentrations of evaporative groundwater loss (Fig. 2a). There is also significant groundwater upwelling and evaporation in Meridiani Planum and the surrounding Arabia Terra region, and an isolated location in the southern highlands. Similar results are found for the post-Tharsis model (Fig. 2b), with the exception that the water table is deeper in the Tharsis region as a result of the higher topography there, and there is more extensive groundwater upwelling in the southern highlands. When the growth of Tharsis is included in the model, the lag between Tharsis construction and BPT migration results in a lowering of the water table in the Tharsis region and to a lesser extent in the surrounding southern highlands, preventing groundwater upwelling in these regions (Fig. 2c).

The predicted locations of groundwater upwelling in the northern lowlands and large impact basins would have been largely buried beneath the subsequent sedimentary, volcanic and aeolian material that forms the Hesperian plains. However, outcrops of layered deposits have been identified in the Hellas, Isidis and Argyre basins, and along the dichotomy boundary near Aeolis Mensa[25] (Fig. 2d). In all three models, Meridiani Planum is one of the only regions of currently exposed Noachian-aged crust for which the model predicts
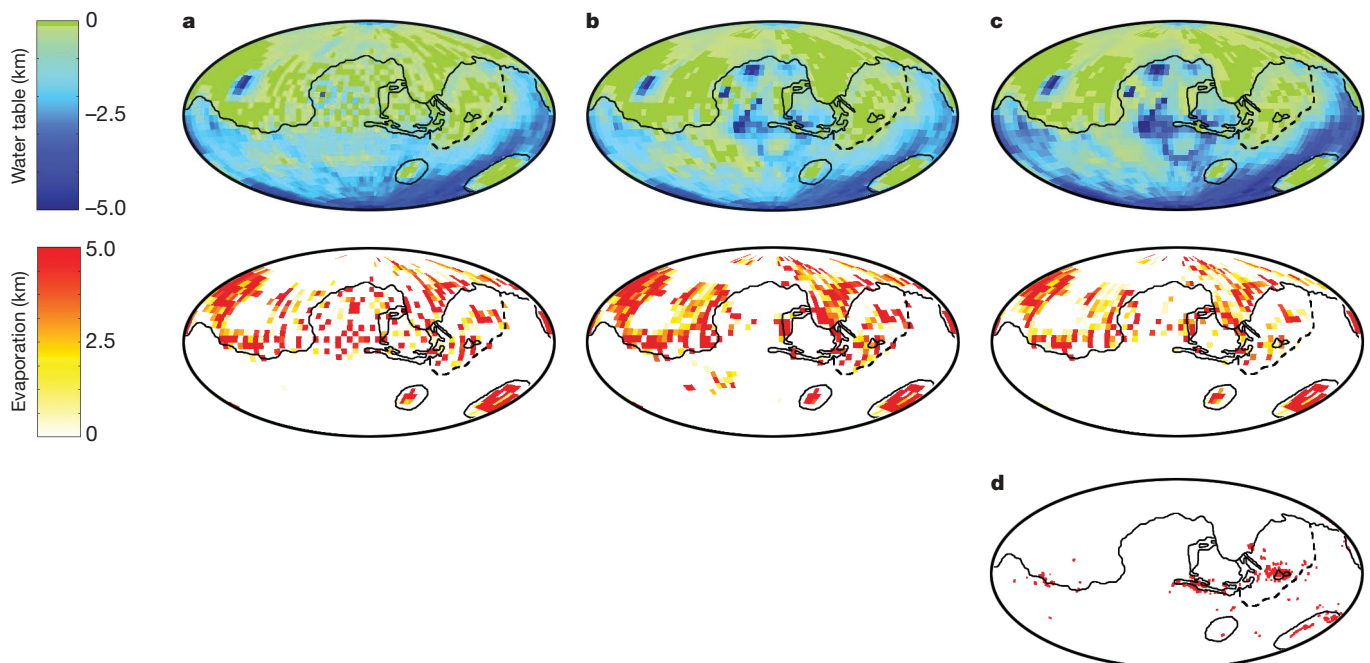

Figure 2 | Modelled hydrologic evolution, and outcrops of layered deposits. a–c, Depth to the water table (top) and cumulative evaporative groundwater loss (bottom); colour scales apply to **a–c**. Results shown after 500 Myr for models assuming pre-Tharsis conditions (**a**), post-Tharsis conditions (**b**) and a steady rate of Tharsis formation (**c**). **d,** The locations of observed outcrops of ancient sedimentary deposits[25] are shown for comparison.

groundwater upwelling and evaporation. The integrated flux to the surface over 500 Myr is equivalent to evaporation of a 2.5-km column of water over a broad area. Increasing the hydraulic conductivity by a factor of 2–5, well within the uncertainty[22], results in similar patterns of upwelling, with 5.4–17 km of evaporation at Meridiani. Assuming that evaporites account for 60% of the deposits[4], their estimated 200–800 m thickness[13,21] would require evaporation of 8–32 km of terrestrial sea water[26]. Fluids deep within the Earth's crust have greater ionic strengths[27] (by a factor of ~3), reducing the amount of water required to ~2.7–11 km, in agreement with the model results.

Although the groundwater fluxes and evaporation rates predicted by the models are small (~10 μm per year), they reflect averaged rates over geologic timescales and large spatial scales. Processes such as local tectonism, volcanic and hydrothermal activity, local-scale precipitation and groundwater flow, climatic fluctuations, variable erosion or deposition rates, or episodic Tharsis formation could modulate this long-term regional groundwater flux. The resulting instantaneous local rates of upwelling could be orders of magnitude greater. The detailed morphology of the deposits would have resulted from the interaction of the regional groundwater upwelling with the local topography and micro-environments at the surface, leading to runoff, ponding, cementation or diagenesis. As the deposits thickened, the water table would rise to remain at or near the surface. Similarly, layered outcrops observed elsewhere[25] may have resulted from groundwater cementation of aeolian or pyroclastic deposits.

To understand the root cause of the groundwater upwelling at Meridiani Planum, we note that it is located near the southern edge of Arabia Terra (Fig. 1). In contrast to the sharp break in slope observed elsewhere along the dichotomy boundary, Arabia Terra is a broad bench perched at intermediate elevation, flanked by steeper slopes leading to the northern lowlands and southern highlands[15,18] (Fig. 3a). For the simplified case of steady, one-dimensional, topography-driven flow in an unconfined aquifer, the discharge is proportional to the product of the height of the water table above the base of the aquifer and the flow velocity, which in turn is proportional to the topographic slope. Conservation of discharge requires that a decrease in slope, and the attendant decrease in flow velocity, will require an increase in the height of the water table above the base of the aquifer, possibly leading to situations in which the water table attempts to rise above the surface. In the model, this excess groundwater upwelling is balanced by evaporation, returning the water table to the surface. Figure 3b presents a cross-section of the topography, water table elevation, and cumulative evaporative groundwater loss from the model along a great circle passing through Meridiani Planum. Immediately below the first break in slope, at the location of the Meridiani deposits, the water table intersects the surface, resulting in substantial evaporative loss. A similar situation occurs below the second break in slope leading down to the northern lowlands. The intersection of the water table with the surface in Arabia Terra is facilitated by its low topography relative to the highlands, leading to scattered sites of groundwater upwelling and isolated sedimentary deposits throughout this region[21,25,28].

The work presented here sheds light on a previously recognized conundrum regarding the Meridiani evaporites. Terrestrial non-marine evaporites commonly result from the ponding and evaporation of meteoric water within an enclosed or restricted basin, concentrating the solutes leached from rocks over the entire drainage basin within a relatively smaller area[29]. However, no such basin exists in association with the Meridiani deposits[13]. The present results suggest that the Meridiani evaporites formed as a result of sustained groundwater upwelling over a broad region driven by global-scale flow. This groundwater would have leached the solutes from large volumes of aquifer material over a range of depths, before reaching Meridiani and concentrating the solutes at the surface to produce thick deposits of evaporites in the absence of a topographic basin. A small-scale terrestrial analogue is found in the Great Artesian Basin of Australia[30], in which the migration of groundwater over hundreds of kilometres produces local evaporite deposits where the water is released to the surface.

Global mineralogical mapping[6] suggests that Mars experienced a wet period dominated by phyllosilicate formation in the early Noachian, followed by more arid and acidic conditions in the late Noachian and early Hesperian in which the evaporitic sulphate deposits formed. During the earlier wet period, surface runoff and the shallow subsurface hydrology probably masked the signature of the slower, global-scale deep hydrology. The resultant aqueous geochemistry would have been dominated by low-temperature water–rock reactions at the surface, consistent with the observed phyllosilicates. The transition to more arid conditions would have led to the pre-eminence of the global-scale deep groundwater flow over the waning shallow hydrology, with the water chemistry determined by moderate- to high-temperature water–rock reactions at depth, leading to a distinct change in the chemical nature of the surface fluids. Hydrological activity would then be focused in regions of upwelling, with the groundwater interacting with the local surface environment to form the deposits at Meridiani Planum.
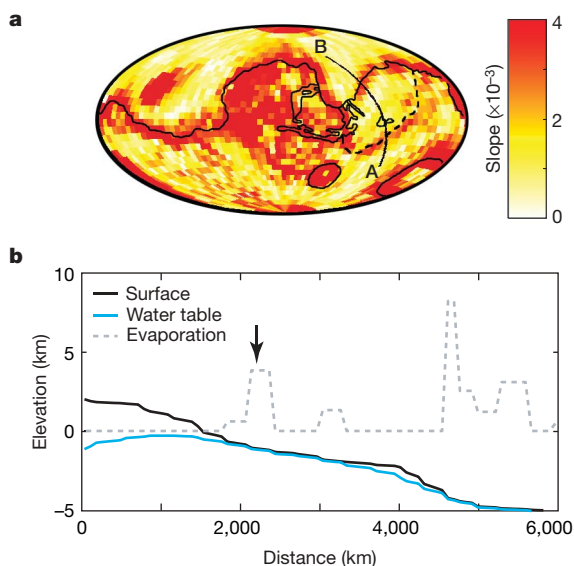
Figure 3 | Role of slopes in driving groundwater upwelling. a, Global slope map of Mars measured at a resolution of 5° per pixel. **b**, Profile of the topography, water table, and the cumulative equivalent column of evaporitic groundwater loss at the end of the Noachian for the steady Tharsis formation model along a great circle path taken parallel to the regional slope in Arabia Terra (line A–B in **a**). The arrow represents the location of Meridiani Planum along the profile. Downturn in the water table at 0 km is a result of the proximity of the Hellas basin.

1.   Squyres, S. W. *et al.* Two years at Meridiani Planum: Results from the Opportunity rover. *Science* **313**, 1403–1407 (2006).
2.   Squyres, S. W. *et al.* Overview of the Opportunity Mars Exploration Rover mission to Meridiani Planum: Eagle Crater to Purgatory Ripple. *J. Geophys. Res.* **111**, E12S12, doi:10.1029/2006JE002771 (2006).
3.   Grotzinger, J. P. *et al.* Stratigraphy and sedimentology of a dry to wet eolian depositional system, Burns formation, Meridiani Planum, Mars. *Earth Planet. Sci. Lett.* **240**, 11–72 (2005).
4.   McLennan, S. M. *et al.* Provenance and diagenesis of the evaporite-bearing Burns formation, Meridiani Planum, Mars. *Earth Planet. Sci. Lett.* **240**, 95–121 (2005).
5.   Arvidson, R. E. *et al.* Nature and origin of the hematite-bearing plains of Terra Meridiani based on analyses of orbital and Mars Exploration Rover data sets. *J. Geophys. Res.* **111**, E12S08, doi:10.1029/2006JE002728 (2006).
6.   Bibring, J. P. *et al.* Global mineralogical and aqueous Mars history derived from OMEGA/Mars Express data. *Science* **312**, 400–404 (2006).
7.   Pollack, J. B., Kasting, J. F., Richardson, S. M. & Poliakoff, K. The case for a wet, warm climate on early Mars. *Icarus* **71**, 203–224 (1987).
8.   Hynek, B. M. & Phillips, R. J. New data reveal mature, integrated drainage systems on Mars indicative of past precipitation. *Geology* **31**, 757–760 (2003).

9. Baker, V. R. & Partridge, J. B. Small martian valleys: Pristine and degraded morphology. *J. Geophys. Res.* **84,** 3561–3572 (1986).
10. Williams, R. M. E. & Phillips, R. J. Morphometric measurements of martian valley networks from Mars Orbiter Laser Altimeter (MOLA) data. *J. Geophys. Res.* **106,** 23737–23751 (2001).
11. Harrison, K. P. & Grimm, R. E. Groundwater-controlled valley networks and the decline of runoff on early Mars. *J. Geophys. Res.* **110,** E12S16, doi:10.1029/2005JE002455 (2005).
12. Hartmann, W. K. & Neukum, G. Cratering chronology and the evolution of Mars. *Space Sci. Rev.* **96,** 165–194 (2001).
13. Hynek, B. M., Arvidson, R. E. & Phillips, R. J. Geologic setting and origin of the Terra Meridiani hematite deposit on Mars. *J. Geophys. Res.* **107,** 5088, doi:10.1029/2002JE001891 (2002).
14. Phillips, R. J. & Hynek, B. M. THEMIS and MOLA provide 3-D stratigraphy in the Terra Meridiani region of Mars. *Eos* 86(*Fall Meet.*), abstr. P24A–04 (2005).
15. Smith, D. E. *et al.* Mars Orbiter Laser Altimeter (MOLA): Experiment summary after the first year of global mapping of Mars. *J. Geophys. Res.* **106,** 23689–23722 (2001).
16. Solomon, S. C. & Head, J. W. Evolution of the Tharsis province of Mars—The importance of heterogeneous lithospheric thickness and volcanic construction. *J. Geophys. Res.* **87,** 9755–9774 (1982).
17. Phillips, R. J., Sleep, N. H. & Banerdt, W. B. Permanent uplift in magmatic systems with application to the Tharsis region of Mars. *J. Geophys. Res.* **95,** 5089–5100 (1990).
18. Zuber, M. T. *et al.* Internal structure and early thermal evolution of Mars from Mars Global Surveyor topography and gravity. *Science* **287,** 1788–1793 (2000).
19. Phillips, R. J. *et al.* Ancient geodynamics and global-scale hydrology on Mars. *Science* **291,** 2587–2591 (2001).
20. Lane, M. D., Christensen, P. R. & Hartmann, W. K. Utilization of THEMIS visible and infrared imaging data for crater population studies of the Meridiani Planum landing site. *Geophys. Res. Lett.* **30,** 1770, doi:10.1029/2003GL017183 (2003).
21. Edgett, K. S. The sedimentary rocks of Sinus Meridiani: Five key observations from data acquired by the Mars Global Surveyor and Mars Odyssey orbiters. *Mars* 1, doi:10.1555/mars.2005.0002 (2005).
22. Hanna, J. C. & Phillips, R. J. Hydrological modeling of the Martian crust with application to the pressurization of aquifers. *J. Geophys. Res.* **110,** E01004, doi:10.1029/2004JE002330 (2005).
23. Deming, D., Nunn, J. A. & Evans, D. G. Thermal effects of compaction-driven flow from overthrust belts. *J. Geophys. Res.* **95,** 6669–6683 (1990).
24. Banerdt, W. B. Support of long-wavelength loads on Venus and implications for internal structure. *J. Geophys. Res.* **91,** 403–419 (1986).
25. Malin, M. P. & Edgett, K. S. Ancient sedimentary rocks of early Mars. *Science* **290,** 1927–1937 (2000).
26. Handford, C. R. in *Evaporites, Petroleum, and Mineral Resources* (ed. Melvin, J. L.) 1–66 (Elsevier, New York, 1991).
27. Moller, P. *et al.* Paleofluids and recent fluids in the upper continental crust: Results from the German Continental Deep Drilling Program (KTB). *J. Geophys. Res.* **102,** 18233–18254 (1997).
28. Hynek, B. M. Implications for hydrologic processes on Mars from extensive bedrock outcrops throughout Terra Meridiani. *Nature* **431,** 156–159 (2004).
29. Smoot, J. P. & Lowenstein, T. K. in *Evaporites, Petroleum, and Mineral Resources* (ed. Melvin, J. L.) 189–347 (Elsevier, New York, 1991).
30. Habermehl, M. A. The Great Artesian Basin, Australia. *J. Austr. Geol. Geophys.* **5,** 9–38 (1980).